

TECHNIQUES FOR REDUCING THE EFFECT OF MEASUREMENT ERRORS IN NEAR-FIELD ANTENNA MEASUREMENTS

Allen C. Newell, Greg Hindman

*Nearfield Systems Inc.
19730 Magellan Drive, Torrance CA 90502, USA
allen_newell@qwest.net*

Keywords: Measurements, Error Analysis, Near-Field Measurements, Corrections.

Abstract

The NIST 18 term error analysis has been used for some time to estimate the uncertainty in the far-field antenna parameters determined from near-field measurements. Each of the error terms is evaluated separately to estimate the uncertainty it produces in parameters such as gain, directivity, side lobe level, cross polarization level and beam pointing angle. This identification and evaluation of uncertainties has led to the development of procedures that can be used to reduce the effect of individual error sources and therefore improve the reliability of the results.

Automated, real time systems have been added to the measurement hardware and electronics that can reduce the effect of such things as probe position errors and cable flexing. Measurement and special computer processing techniques have also been developed to self-calibrate and correct for transmission path differences of dual mode probes.

More recently, a number of techniques have been developed that provide a means to reduce the effect of measurement errors without the need of special hardware or additional measurements. These procedures often involve additional data processing steps to identify and reduce the presence of the error in the measured data, but the processing time is small and the improvement in some parameters can be very significant. In some cases, the error signal level can be reduced by 10 to 20 dB. Such techniques have been developed for errors due to bias error leakage in the receivers, non-ideal rotary joints, spherical rotator misalignment, and room scattering. Further improvements can be realized by making additional measurements to reduce multiple reflection effects, position errors and room scattering in spherical systems.

Examples of these techniques will be presented to illustrate the methods and demonstrate typical improvement.

1 Introduction

The total estimated uncertainties in antenna parameters such as gain, side lobe level, cross polarization level, and beam pointing determined from near-field measurements are derived using a procedure referred to as the NIST 18 Term Error Analysis¹. The contributions for each of the 18 terms are estimated using a combination of analysis, self comparison measurements and simulation and then they are combined using an RSS process. For example, multiple reflections between the AUT and the probe can produce errors in all of the far-field parameters, and it is evaluated by acquiring data at a sequence of Z-distances in steps of $\lambda/8$. The far-field patterns for each data set are calculated and then averaged to reduce the effect of the multiple reflections. Comparing a single far-field to the average gives an estimate of this error source as illustrated in Figure 1.

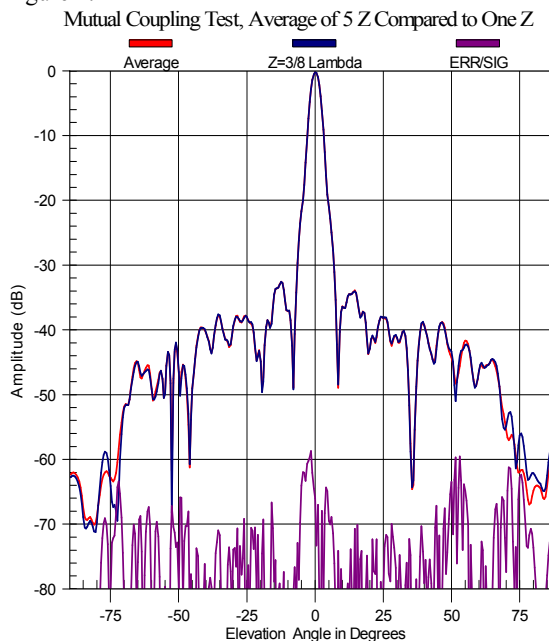


Figure 1 Example of results of multiple reflection test for planar near-field measurements.

From the pattern comparison graphics like Figure 1, we can estimate an “Signal to Error” ratio shown by the lower curve. This represents an equivalent error signal level for this single source of uncertainty in the measurement process. This can be converted to an uncertainty in a given parameter by using the following equation.

$$ERROR / Signal = E / S = 20 * \log \left[10^{\left(\frac{\Delta_{dB}}{20}\right)} - 1 \right] \quad (1)$$

$$Error \text{ in dB} = \Delta_{dB} = 20 * \log \left[1 + 10^{\left(\frac{E/S}{20}\right)} \right]$$

For instance, if a single near-field measurement was obtained for the AUT/Probe/measurement system used to obtain the data in Figure 1, the peak error signal of -60 dB relative to the beam peak would be 20 dB below a -40 dB side lobe and the peak uncertainty in any -40 dB side lobe would be 0.8 dB.

Another result of identifying and estimating the effect of individual measurement errors has been the development of correction techniques for some of the terms. These techniques can use either additional information about the measurement system such as a Z-position error map or additional near-field data to reduce the uncertainty of individual terms. For instance in the case of multiple reflections, the average of far-fields from five different Z-distances would have a smaller uncertainty than a single result. In some cases, corrections can be derived without additional measurements. The following paper will describe and illustrate some of these correction techniques for planar and spherical near-field measurements.

Table 1 Near-Field Corrections.

Correction Technique	Far-Field Parameters Affected
Multiple Reflections Planar and Spherical	Gain, Side lobe, Cross Pol, Pointing
AUT Alignment Planar and Spherical	Pointing Pattern comparisons
X, Y and Z Position Errors Planar	Gain, Side lobe, Cross Pol, Pointing
Rotator Alignment and position Errors Spherical	Gain, Side lobe, Cross Pol, Pointing
Drift Correction Planar and Spherical	Gain, Pointing
Flexing Cable Planar	Gain, Side lobe, Cross Pol, Pointing
Probe Rotary Joint Spherical	Gain, Side lobe, Cross Pol, Pointing
Room Scattering Spherical	Gain, Side lobe, Cross Pol, Pointing
Impedance Mismatch Planar and Spherical	Gain
Bias Error Leakage Planar	Gain, Cross Pol, Pointing

The correction techniques that will be covered in this paper are summarized in Tables 1 . In addition to the listed items, correction for the gain, pattern and polarization of the probe are included as a standard part of the data processing. A network correction can also be applied for dual port probes to account for different transmission lines between the ports and receiver. These will not be considered in detail here since they are routinely applied and well understood.

2 Description and examples of the correction techniques

Multiple Reflections Planar and Spherical. To correct for multiple reflections between the AUT and probe, complete near-field measurements are taken at a series of Z-positions separated by $\lambda/8$. The far-fields are calculated for each and then averaged.

AUT alignment Planar and Spherical. When the AUT is not precisely aligned to the reference coordinate system, the patterns can be rotated mathematically. Vector components and or coordinate angles may change for some rotations and this correction must be used carefully when comparing with measurements on a different range.

Position Errors Correction Planar and Spherical. This correction can take different forms. The precise position of the probe can be monitored during the measurement process with laser optics and the probe can be moved in X, Y and Z to correct for deviations from the ideal surface and raster coordinates. The probe motion can also be recorded with an optical system and the information stored in the measurement computer. This information can be used to mechanically correct for the position errors during measurements or applied as an approximate mathematical correction during processing².

Rotator Alignment for Spherical. This is a special case of position error correction. The orthogonality and intersection of the theta and phi axes and the coincidence of the phi and probe polarization axes can be checked by measuring and comparing near-field cuts at $\theta = 0$ and 180 degrees. An example of this process is shown in Figure 2. The slope of the amplitude difference between the $\phi = 0$ and $\phi = 180$ degree cuts is a precise measure of the θ -zero setting of the angular encoder. An NSI script has been developed to automatically acquire and/or process the near-field data; compare the two cuts; fit the amplitude and phase difference curves and derive the θ -zero and the non-intersection errors. For the data in Figure 2, the θ -zero setting was within recommended tolerance of 0.05 degrees. The corresponding phase difference processing determines the non-intersection error and recommends the mechanical adjustment to make a correction. With this automated measurement and processing, the alignment converges quickly. If near-field data has already been acquired with small alignment errors, an approximate correction can be applied using the

corrections recommended by the alignment script and a mathematical model derived from previous error simulations.

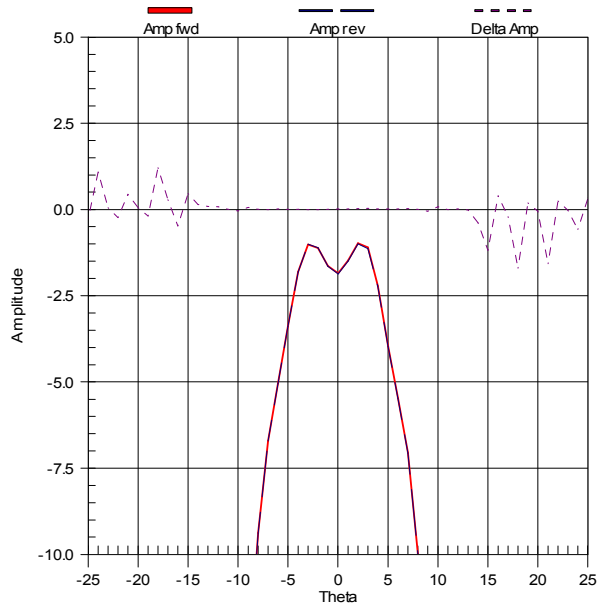


Figure 2 Results of spherical alignment processing script. Near-field amplitude cuts and difference.

Drift for Planar and Spherical Thermal drift during measurements can cause changes in the transmission lines and electronic components as well as the alignment of the AUT. These can be correct by periodically returning to one or more reference point on the measurement grid and recording the amplitude and phase of the probe output as described in the NSI developed MTI technique. Numerical correction is then applied to the measured data³.

Flexing Cable Correction for Planar. The RF cables connecting the moving probe to the source or receiver will introduce some amplitude and phase variation as it is moved. Like the position correction, the cable variations can be measured and stored for future correction or in some cases the variations and corrections are recorded and applied^{4 5} during measurements.

Probe Rotary Joint Correction for Spherical. The rotary joints associated with the theta and phi rotators produce an effect similar to the flexing cable in planar measurements and can be treated in a similar way. They produce small variations as a function of theta and phi that usually have little effect on the far-field patterns. The rotary joint used for the probe polarization can have a more serious affect since it is rotated to just two positions and all of the data for one component has the same error applied. A correction can be obtained from the measured data by comparing the amplitudes and phases of the two components at (θ, ϕ) coordinates, $(0,0)$, $(0,90)$, $(0,180)$, $(0,270)$, $(0,360)$. From knowledge of the AUT and probe polarizations we can identify the points where the amplitudes should be identical and the phases should be either identical or 180 degrees different. From the measured values at these points, a constant correction can be determined and applied to

all the data for one component. This correction is more important at high frequencies where rotary joints may not be as accurate.

Impedance Mismatch Correction. To obtain gain, EIRP or saturating flux density results from near-field data, a gain standard is required and one or more transmission lines must be moved from the AUT or probe to the gain standard. The different power transfer between the transmission line and the antennas can be accounted for by measuring the complex impedance of each device and applying a calculated correction. This correction does not affect relative patterns, polarization or beam pointing.

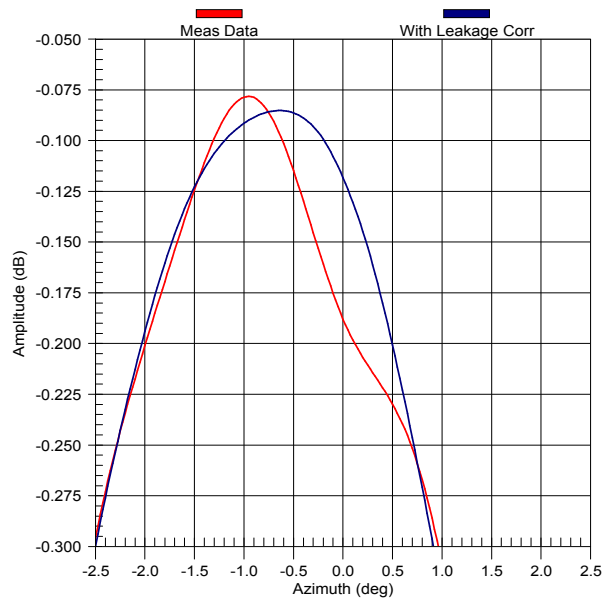


Figure 3 Example of bias error leakage effect on the far-field peak for a standard gain horn measurement.

Bias Error Leakage for Planar. The detection and conversion of the RF signals to real and imaginary or amplitude and phase components in the receivers introduces a small bias error that produces a very small constant signal on the recorded amplitude and phases of the near-field pattern. This signal may be 50 to 100 dB below the peak near-field amplitude, but in the FFT processing of the data for planar measurements, the leakage signal is summed coherently in the on-axis direction. It can produce a noticeable distortion in the main beam region if the measurement area is much larger than the AUT area as shown in Figures 3 and 4 for a standard gain horn measurement. This can have a significant impact on gain measurements especially if there is also a noticeable multiple reflection or room scattering interference in the gain horn data. The amplitude and phase of the bias error can be determined from the data without additional measurements⁶. Scripts have been developed to use the measured data at the extremes of the measurement area where the amplitude is small. In this region, the sum of the data will converge to the constant bias error and it can then be subtracted from the measured data⁷. The data shown in Figures 3 and 4 were

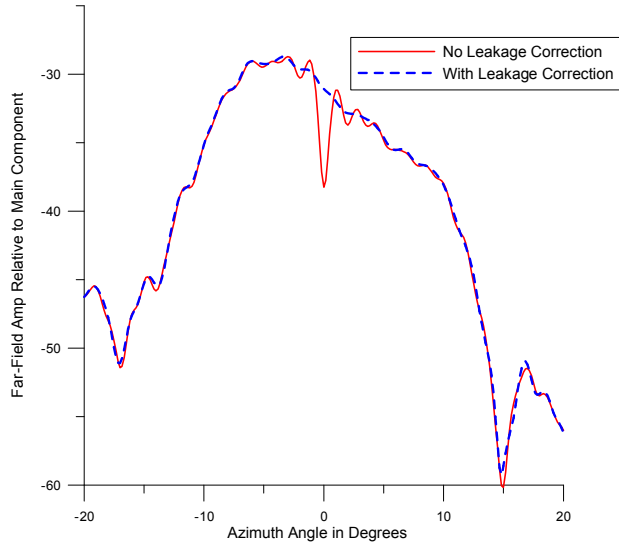


Figure 4 Example of bias error leakage on cross component data.

corrected in this way to greatly reduce the effect of the bias error leakage signal.

Bias error leakage has no effect on spherical data since a constant signal over the sphere does not produce or modify any of the calculated spherical modes.

Room Scattering Correction for Spherical. Scattering from structures and absorber in a planar near-field range introduces an error that is generally small for directive antennas. It is also difficult to estimate this error, partly because it is small and because the procedure is demanding and time consuming.

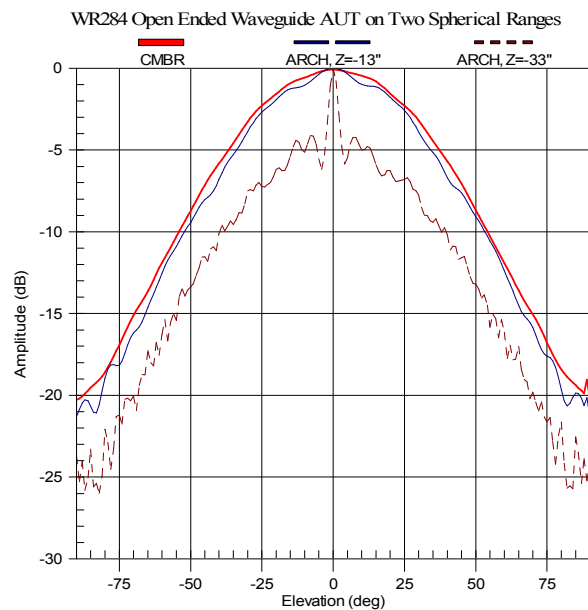


Figure 5 Far field patterns of an Open Ended Waveguide probe measured on three different spherical near-field ranges

The AUT and probe must be translated together in a combination of X, Y and Z movements while maintaining precise angular alignment. The translations should be at least multiple wavelengths in dimension and this generally means that the AUT must be realigned in the new position. Comparison of the patterns from the two locations provides an estimate of the room scattering but it is difficult to distinguish from alignment differences, probe/AUT multiple reflections and system drift. There is no practical way to correct for room scattering in planar measurements since this would require multiple repositioning of the AUT and probe.

The room scattering effect for spherical measurements can be more severe when low gain AUT's are being measured as illustrated in Figure 5. An Open Ended Waveguide (OEWG) probe was the AUT in two positions on an arch range with no absorber enclosing the scanner as shown in Figure 6 and in an anechoic chamber. The effect of scattering is very evident in the two curves from the arch range as shown in Figure 5.



Figure 6 OEWG probe on the arch spherical range without absorber enclosure.

For spherical measurements where scattering may be a problem, techniques have been developed⁸ that can reduce the effect of room scattering for some situations. The MARS technique developed by NSI uses the following measurement and processing steps and a similar procedure is used in another technique⁹. The AUT is oriented with its nominal phase center translated from the origin of the spherical coordinate system by at least 2 wavelengths. The spherical near-field data is over sampled by a factor of two and the usual near-field data acquired. Graphics produced during the subsequent processing will indicate if the over sampling is

sufficient or excessive. The actual location of the AUT phase center is determined as the first step in the processing by fitting the far-field phase patterns in the region of the main beam. The far-field pattern is calculated from the measured data and a phase correction is applied to effectively translate the AUT so its phase center is at the origin. This translated far-field pattern is copied to the near-field and replaces the original measured data. The new data is again processed through the spherical transform software and a filter is applied to remove the higher order modes that are inconsistent with the AUT's physical dimensions. Room scattering that is contained in these higher order modes is therefore eliminated from the final results. Room scattering that is contained in the lower order modes will not be removed and remains in the far-field pattern. Numerous tests have shown that for low and medium gain antennas, room scattering effects can be reduced by approximately 10 dB with this process as shown in Figure 7. When the room scattering levels are very small, such as for a directive AUT in a reasonably good chamber, the improvement may be small because the error level is already so low.

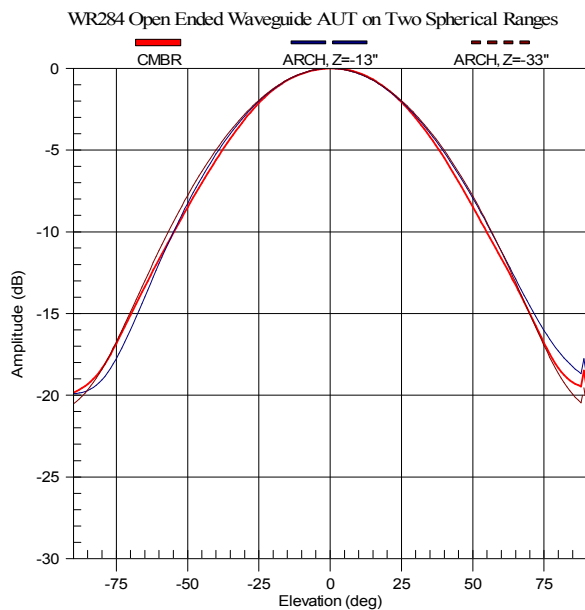


Figure 7 OEWG far-field patterns from three measurements after MARS processing.

3 Summary

Correction techniques for planar and spherical near-field measurements have been described and illustrated with typical data. These can improve the accuracy of results and in some cases do not require any additional data or near-field measurements. In most cases, the analysis and additional data processing has been automated with user-friendly scripts. They have been applied in a number of measurements on low medium and high gain antennas and at frequencies from 500 MHz to 60 GHz.

As an example of what can be achieved with careful measurements and application of the appropriate corrections, Figure 8 shows the results of a recent comparison between a planar and spherical near-field range.

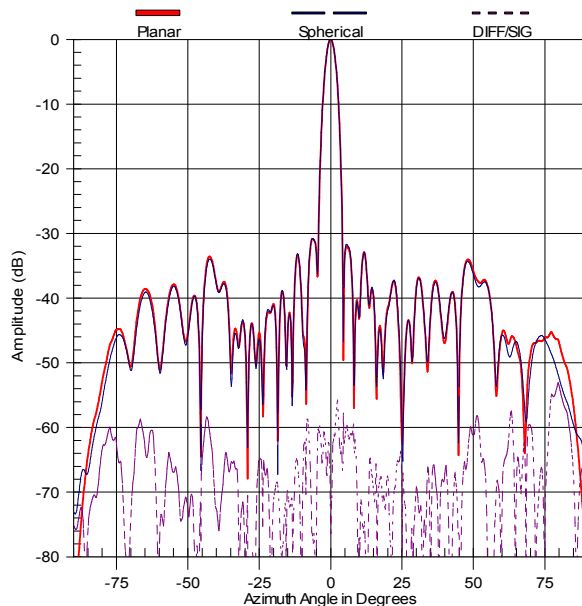


Figure 8 Pattern comparison between planar and spherical near-field measurements.

References

- ¹ A. C. Newell, Error analysis techniques for planar near-field measurements, IEEE Trans. Antennas & Propagation, AP-36, p. 581, 1988
- ² Wittmann, R.C., Spherical near-field scanning: determining the incident field near a rotatable probe, IEEE Antenna Propagation Society Symposium Digest, 7-11 May, Vol.1, pp.224-227, Dallas, TX, 1990
- ³ Hindman, G., Slater, D., Thermal Error Corrections in Near-Field Measurements, AMTA Proceedings, Oct. 1995.
- ⁴ Hess, D.W., Principle of the three-cable method for compensation of cable variations, AMTA Symposium Digest, pp.10-26 – 10-31, Columbus, OH, 1992
- ⁵ Tuovinen, J., Lehto, A., Raisanen, A., A new method for correcting phase errors caused by flexing of cables in antenna measurements, IEEE Transactions, AP-39 No.6, June 1991.
- ⁶ Rousseau, P. R., "An algorithm to reduce errors in planar near-field measurement data, AMTA Proceedings, Oct. 1999, pp 269-271.
- ⁷ Newell, A. C., Guerrieri, J., MacReynolds, K., Methods to estimate and reduce leakage bias errors in planar near-field antenna measurements, AMTA Proceedings, Oct. 2002
- ⁸ Hindman, G., Newell, A.C., Reflection suppression in a large spherical near-field range, AMTA Symposium Digest, pp.270-275, Newport, RI, 2005
- ⁹ Hess, D.W. The *IsoFilter™* technique: isolating an individual radiator from spherical near-field data measured in a contaminated environment, Postdeadline Submissions, AMTA Symposium, Austin, TX, 2006